ANN Prediction Models for Outdoor SIMO Millimeter Band System

Nektarios Moraitis[1] and Demosthenes Vouyioukas[2]
1 Mobile Radiocommunications Laboratory, National Technical University of Athens, 9 Heroon Polytechniou str. 15773, Zografou, Athens, Greece, morai@mobile.ntua.gr
2 Dept. of Information and Communication Systems Engineering, University of the Aegean, Karlovassi 83200, Samos, Greece
dvouyiou@aegean.gr

Abstract. This paper presents the prediction propagation paths of angle of arrivals (AoAs) of a Smart Antenna System in an outdoor environment utilizing Artificial Neural Networks (ANN). The proposed models consist of a Multilayer Perceptron and a Generalized Regression Neural Network trained with measurements of an antenna system consisted of a Single Input Single Output (SISO) system in the millimeter wave band. For comparison purposes the theoretical Gaussian scatter density model was investigated for the derivation of the power angle profile. The proposed models utilize the characteristics of the environment for prediction of the angle of arrivals of each one of the propagation paths and can be applicable for the derivation of SIMO (Single Input Single Output) parameters, such as system capacity. The results are presented towards the average error, standard deviation and mean square error compared with the measurements and they are capable for the derivation of accurate prediction models for the case of AoA in an outdoor millimeter wave propagation environment.

1 Introduction

Smart Antenna Systems [1] and especially MISO (Multiple Input Single Output) [2] or SIMO (Single Input Multiple Output) [3] systems have already been evaluated for the optimization of wireless system performance. The prediction of the field strength is a very complex and difficult task. In most cases, there are no clear line-of-sight (LOS) conditions between the transmitter and the receiver. Generally, the prediction models are classified as empirical [4] or theoretical [5], or a combination of these two [6]. However, the main problem of the classical empirical models is the unsatisfactory accuracy, while the theoretical models lack in computational efficiency.

During last years, Artificial Neural Networks (ANN) have experienced a great development. ANN applications are already very numerous. Classificators, signal processors, optimizers and controllers have already been realized. Although there are several types of ANN's all of them share the following features [7]: exact analytical formula impossible; required accuracy around some percent; medium quantity of data to process; environment adaptation that allows them to learn from a changing environment and parallel structure that allows them to achieve high computation speed. All these characteristics of ANN's make them suitable for predicting field strength in different environments and additionally angle of arrivals (AoA).

The prediction of field strength and AoA can be described as the transformation of an input vector containing topographical and morphographical information (e.g. path profile) to the desired output value. The unknown transformation is a scalar function of many variables (several inputs and a single output), because a huge amount of input data has to be processed. The inputs contain information about the transmitter and receiver locations, surrounding buildings, frequency, etc while the output gives the propagation loss for those inputs. From this point of view, research in propagation loss modeling consists in finding both the inputs and the function that best approximate the propagation loss. Given that ANN's are capable of function approximation, they are useful for the propagation loss and angle of arrival modeling. The feedforward neural networks are very well suited for prediction purposes because do not allow any feedback from the output (field strength or path loss) to the input (topographical and morphographical data).

In this paper, the presented studies develop a number of Multilayer Perceptron Neural Networks (MLP-NN) and Generalized Radial Basis Function Neural Networks (RBF-NN) based models trained on extended data set of propagation path loss measurements taken in an outdoor environment. The smart antenna measurement system was a SISO one where a continuous wave (CW) signal at 60 GHz was transmitted from a fixed base station to a fixed receiver, comprised of one antenna element, rotated in the azimuthal direction recording the multipath components. The signal envelope as a function of time was recorded. The performance of the neural network based models is evaluated by comparing their prediction, standard deviation and mean square error (MSE) between their predicted values and measurements data. Also, a comparison with the results is obtained by applying the Gaussian model.

The remainder of this paper is organized as follows. Section 2 deals with the ANN overview describing and explaining the behavior of the two NN utilized models. In Section 3, an analytically description of the geometry of the measurement environment under consideration is presented along with the measurement procedure. In Section 4, the NN prediction models are implemented analytically describing the implementation method and the prediction results are presented in terms of measured Power Angle Profile (PAP), taking also into consideration the Gaussian model. Finally, Section 5 is devoted to conclusions derived by the prediction procedure.

2 The ANN Overview

2.1 Multilayer Perceptron Neural Network (MLP-NN)

Fig. 1 shows the configuration of a multilayer perceptron with one hidden layer and one output layer. The network shown here is fully interconnected. This means that each neuron of a layer is connected to each neuron of the next layer so that only forward transmission through the network is possible, from the input layer to the output layer through the hidden layers. Two kinds of signals are identified in this network:

- The function signals (also called input signals) that come in at the input of the network, propagate forward (neuron by neuron) through the network and reach the output end of the network as output signals;
- The error signals that originate at the output neuron of the network and propagate backward (layer by layer) through the network.

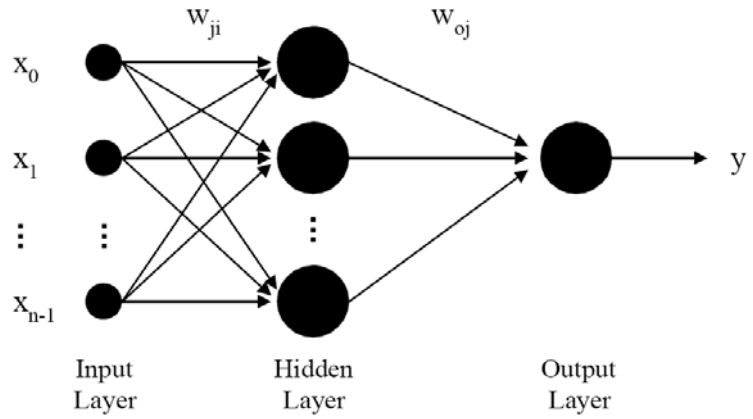

Fig. 1. MLP-NN configuration

The output of the neural network is described by the following equation:

$$y = F_o\left(\sum_{j=0}^{M} w_{0j}\left(F_h\left(\sum_{i=0}^{N} w_{ji}x_i\right)\right)\right) \tag{1}$$

where

- w_{0j} represents the synaptic weights from neuron j in the hidden layer to the single output neuron,
- x_i represents the *i-th* element of the input vector,
- F_h and F_o are the activation function of the neurons from the hidden layer and output layer, respectively,
- w_{ji} are the connection weights between the neurons of the hidden layer and the inputs.

The learning phase of the network proceeds by adaptively adjusting the free parameters of the system based on the mean square error E, described by Equation (2), between predicted and measured path loss for a set of appropriately selected training examples:

$$E = \frac{1}{2}\sum_{i=1}^{m}\left(y_i - d_i\right)^2 \tag{2}$$

where y_i is the output value calculated by the network and d_i represents the expected output.

When the error between network output and the desired output is minimized, the learning process is terminated and the network can be used in a testing phase with test vectors. At this stage, the neural network is described by the optimal weight configuration, which means that theoretically ensures the output error minimization.

2.2 Generalized Radial Basis Function Neural Network (RBF-NN)

The Generalized Radial Basis Function Neural Network (RBF-NN) is a neural network architecture that can solve any function approximation problem. The learning process is equivalent to finding a surface in a multidimensional space that provides a best fit to the training data, with the criterion for the "best fit" being measured in some statistical sense. The generalization is equivalent to the use of this multidimensional surface to interpolate the test data.

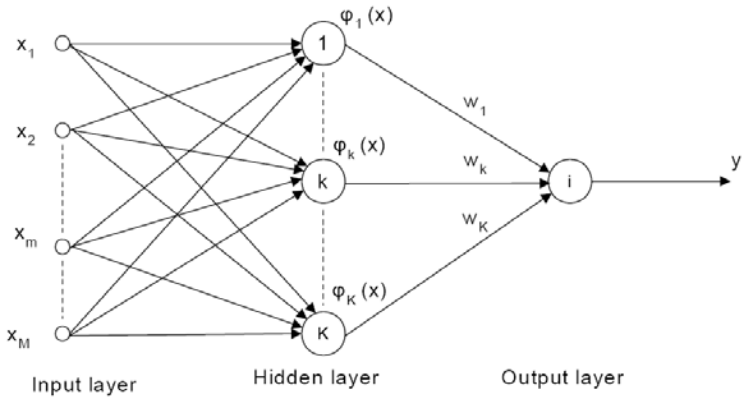

Fig. 2. RBF-NN architecture

As it can be seen from Fig. 2, the Generalized Radial Basis Function Neural Network (RBF–NN) consists of three layers of nodes with entirely different roles:

- the input layer, where the inputs are applied,

- the hidden layer, where a nonlinear transformation is applied on the data from the input space to the hidden space; in most applications the hidden space is of high dimensionality and
- the linear output layer, where the outputs are produced

The most popular choice for the function φ is a multivariate Gaussian function with an appropriate mean and autocovariance matrix. The outputs of the hidden layer units are of the form:

$$\varphi_k\left[x\right] = \exp\left[-\frac{\left(x - v_k^x\right)^T \left(x - v_k^x\right)}{2\sigma^2}\right] \tag{3}$$

when v_k^x are the corresponding clusters for the inputs and v_k^y are the corresponding clusters for the outputs obtained by applying a clustering technique of the input/output data that produces K cluster centers [8]. v_k^x and v_k^y are defined as:

$$v_k^x = \sum_{x(p)\in\text{cluster k}} x(p) \tag{4}$$

$$v_k^y = \sum_{y(p)\in\text{cluster k}} y(p) \tag{5}$$

The outputs of the hidden layer nodes are multiplied with appropriate interconnection weights to produce the output of the GRNN. The weight for the hidden node k (i.e., w_k) is equal to:

$$w_k = \frac{v_k^x}{\sum_{k=1}^{K} N_k \exp\left[-\frac{d\left(x, v_k^x\right)^2}{2\sigma^2}\right]} \tag{6}$$

where N_k is the number of input data in the cluster centre k, and

$$d\left(x, v_k^x\right) = \left(x - v_k^x\right)^T \left(x - v_k^x\right) \tag{7}$$

3 Measurement Environment and Procedure

The measurement took place in a typical urban environment as indicated in Fig. 3. The ground plan is illustrated as well as the transmitter and receiver positions. The first receiver position is 30 m away from the transmitter, whereas the second location is 70 m apart. Both transmitter and receiver terminals were placed at 3 m above the ground. Line-of-Sight (LoS) condition was preserved during the measurement. The street where the measurement took place is 20 m wide, including the pavements. All

the indicated buildings have 5 to 6 stories creating a narrow propagation canyon. The buildings are made with concrete and bricks, while all the building facades are covered with plaster and paint. There were also cars parked along both sides of the road, but their height is lower than the direct propagation path between the transmitter and receiver.

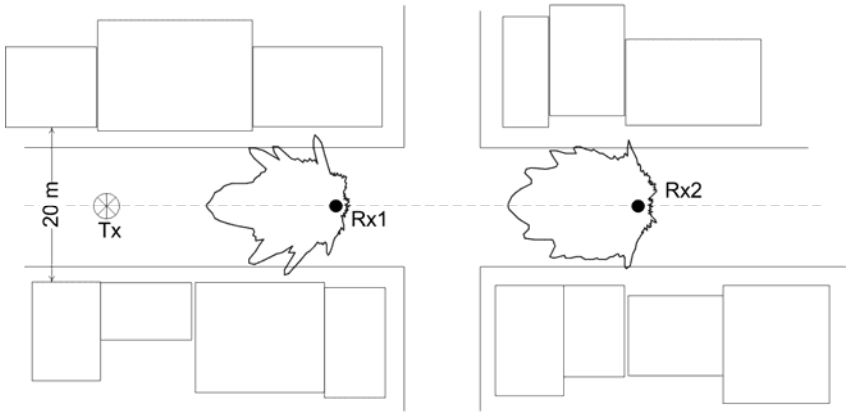

Fig. 3. Measurement environment and superimposed the derived Power Angle Profile.

The measurements were performed by transmitting a continuous wave (CW) signal at 60 GHz, from a fixed base station to a fixed receiver, and recording the signal envelope as a function of time. Details for the measurement setup can be found in [9]. The transmitter output power was 100 mW (+20 dBm). The receiver hardware is located on a trolley, which was stationary at the measurement position. After amplification, the received signal is down-converted to 300 MHz IF and fed to a commercial receiver. The input to the automatic gain control (AGC) of the receiver is then sampled at 2 kHz and the data values were stored to a portable PC. The receiver had a noise floor of -90 dBm. For this measurement, a biconical antenna (omni-directional with 0 dBi gain in azimuth and 36^o in elevation) was used as the transmitter antenna, and a horn antenna with 35 dBi gain was used as the receiver antenna. Both antennas are vertically polarized. The half power beamwidth of the horn antenna was 4^o in azimuth and 3^o in elevation. When a highly directional antenna is used, the system provides high spatial resolution to resolve multipath components with different AoAs.

During the measurements, a mechanically steered directional antenna was used to resolve multipath components. An automated system was used to precisely position the receiver antenna along a linear track and then rotate the antenna in the azimuthal direction. At each position, the receiver antenna is rotated in azimuth from 0 to 360^o with a step size of 5^o and power was recorded at each of the 72 angular steps. Then, a local average is calculated from the measurement results at 10 different positions along the linear track being $\lambda/2$ apart. The local average helps to remove any residual small-scale or time-varying fading that may occur at individual

positions. The precisions of the track and spin positions are better than 1 mm and 1^o, respectively.

Consequently, if we know the Power Angle Profile (PAP) of a SISO channel, we can calculate the channel matrix of a SIMO channel multiplying the array response vector at the receiver. The PAP of a SISO channel can be yielded by either PAP measurements between fixed transmit and receive terminals, a properly trained NN model and, a theoretical model (e.g. Gaussian model).

4 Prediction Models' Implementation

The goal of the prediction is not only to produce small errors for the set of training examples but also to be able to perform well with examples not used in the training process. This generalization property is very important in practical prediction situation where the intention is to use the propagation prediction model to determine the angle of arrival of potential transmitter locations for which no or limited measured data are available.

The selection of the set of training examples is very important in order to achieve good generalization properties [7], [10]. The set of all available data is separated in two disjoint sets that are training set and test set. The test set is not involved in the learning phase of the networks and it is used to evaluate the performance of the neural model. An important problem that occurs during the neural network training is the overadaptation that is the network memorizes the training examples and it does not learn to generalize the new situations. In order to avoid overadaptation and to achieve good generalization performances, the training set is separated in the actual training subset and the validation subset, typically 10-20 % of the full training set [7]. In order to make the neural network training process more efficient, the input and desired output values are normalized so that they will have zero mean and unity standard deviation.

Since the purpose is to train the neural networks to perform well for all the routes, we should build the training set including points from the entire set of measurements data. In our applications the neural networks are trained with the Levenberg-Marquardt algorithm, which converges faster than the backpropagation algorithm with adaptive learning rates and momentum. The Levenberg-Marquardt algorithm is an approximation of Newton's method. As an optimization technique is more powerful than the method of gradient descent used in backpropagation algorithm. The Levenberg-Marquardt rule for updating parameters (weights and biases) is given by:

$$\Delta W = \left(J^T J + \mu I \right)^{-1} J^T e \tag{8}$$

where e is an error vector, μ. is a scalar parameter, W is a matrix of networks weights and J is the Jacobian matrix of the partial derivatives of the error components with respect to the weights. For large values of μ the J^TJ terms become negligible and learning progresses according to $\mu^{-1}J^Te$, which is gradient descent. Whenever a step is taken and error increases, μ is increased until a step can be taken without

increasing error. However, if μ becomes too large, no learning process takes place (i.e. $\mu^{-1}J^{T}$e approaches zero). This occurs when an error minima has been found. For small value of μ, the above expression becomes the Gaussian-Newton method.

A data set of 406 patterns, that represents 20% from all available patterns, was used for training purpose. A set of 1620 patterns was used to test the model. In order to train the NN model the measured PAP was used. In Table 1, the average error, the standard deviation and the mean square error are presented, obtained from the training set by the proposed Multilayer Perceptron Neural Network and the Generalized Regression Neural Network. Fig. 4 presents the measured Power Angle Profile (PAP) together with the results derived by the MLP-NN and the RBF-NN predictions. As it is evident the results between the measured and the predicted PAP are very good with the Mean Square Error (MSE) equals to 4.9 dB for the MLP-NN model and 2.6 dB for the RBG-NN model. Furthermore, the theoretical Gaussian model for angular profile prediction is utilized for comparison reasons and presented also in Table 1 and Fig. 4. The Gaussian model is given by [11]:

$$PAP(\phi) = \frac{1}{2\pi\sigma_{\phi}^{2}} \exp\left[-\frac{\phi^{2}}{2\sigma_{\phi}^{2}} \right] \tag{9}$$

The measured angular spread σ_{ϕ} was calculated 240^{o} for the first and 260^{o} for the second measurement position. Hence the same value will be used in Equation (9). The measured angular spread is calculated by [12]:

$$\sigma_{\phi} = \sqrt{1 - \frac{\|F_1\|^{2}}{\|F_2\|^{2}}}, \quad F_n = \int_{0}^{2\pi} p(\theta) \exp(jn\theta) d\theta \tag{10}$$

where F_n (n =1 or 2) is given by [12], and $p(\theta)$ is the measured PAP. The MSE between the measured PAP and the Gaussian model was found equal to 6.4 dB. All the results are summarized in Table 1.

Table 1. Prediction results of the ANN models' implementation

	Model	Average Error [dB]	Standard Deviation [dB]	Mean Square Error [dB]
Rx-1	RBF-NN	2.0	1.3	2.4
	MLP-NN	4.0	2.1	4.5
	Gaussian	5.2	3.2	6.0
Rx-2	RBF-NN	2.5	1.1	2.8
	MLP-NN	4.8	2.0	5.2
	Gaussian	5.5	3.5	6.7

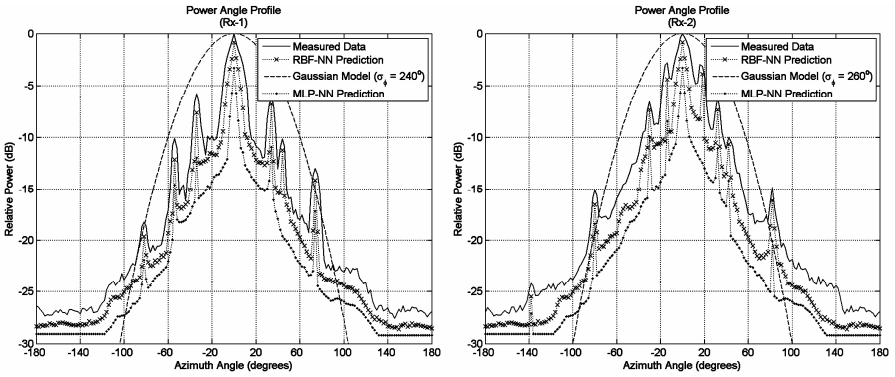

Fig. 4. Comparison between the measured PAP, RBF-NN, MLP-NN prediction, and theoretical Gaussian model for two different receiver's location.

From Fig. 4 it is clear that the prediction of the trained NN models is very good, whereas the best results are yielded by the RBF-NN model. On the other hand the Gaussian model provides greater errors than the other two cases because it is not so accurate, and takes into account a smaller range of azimuth angle.

5 Conclusions

In this paper we examined the applicability of the neural networks for the prediction of angle of arrivals in an outdoor smart antenna system. The data measurements of an outdoor environment using a rotating receiver in the azimuthal direction recording the multipath components at the millimeter wave band of 60 GHz were taken into consideration for training purposes of the NN. Two NN models (RBF and MLP) were considered for the derivation of the prediction models as well as the Gaussian theoretical model is evaluated for comparison purposes. The main advantage of the proposed NN models is that the models should be easily adjusted to specific environments and complex propagation conditions. The knowledge of the Power Angle Profile from the ANN prediction models of a SISO channel can be used for the calculation of the channel matrix of a SIMO channel multiplying the array response vector at the receiver.

The results are depicted in terms of average error, standard deviation and mean square error compared with the measurements and showed very good accuracy. The MSE between the measurements and the NN-models was found 4.9 dB for the MLP-NN model and 2.6 dB for the RBG-NN model. The Gaussian model provides greater errors because it takes into account a smaller range of azimuth angle. High accuracy can be obtained, because the NNs are trained with measurements taking into account buildings characteristics and orientation, thus contain realistic propagation effects considering parameters which are difficult to include in analytic equations. In more specific local cases, the accuracy can be improved by using additional NNs training. Results are always connected with some uncertainty but accuracy is sufficient for prediction purposes.

References

1. J. H. Winters, Smart antennas for wireless systems, *IEEE Personal Commun.*, **5**(1) (1998), 23–27.
2. K. C. Zangi, L.G. Krasny, Capacity-achieving transmitter and receiver pairs for dispersive MISO channels, *IEEE Trans. on Wireless Communications*, **2**(6), 1204 – 1216 (2003).
3. J. K. Tugnait, A multidelay whitening approach to blind identification and equalization of SIMO channels, *IEEE Trans. on Wireless Communications*, **1**(3), 456 – 467 (2002).
4. M. Hata, Empirical formula for propagation loss in land mobile radio services, *IEEE Trans. on Vehicular Technology,* **29**(3), 317-325 (1980).
5. J. Walfisch, H. L. Bertoni, A theoretical model of UHF propagation in urban environments, *IEEE Trans. On Antennas and Propagation,* **36**(12), 1788-1796 (1988).
6. G. K. Chan, Propagation and coverage prediction for cellular radio systems, *IEEE Trans. on Vehicular Technology,* **40**(4), 665-670 (1991).
7. S. Haykin, *Neural Networks: A Comprehensive Foundation*, IEEE Press (McMillan College Publishing Co., 1994).
8. W. Honcharenko, H. L. Bertoni, J. L. Dailing, J. Qian, and H. D. Yee, Mechanisms Governing UHF Propagation on Single Floors in Modern Office Buildings, *IEEE Trans. on Vehicular Technology*, **41**(4), 496-504 (1992).
9. A. Kanatas, N. Moraitis, G. Pantos, and P. Constantinou, Time delay and coherence bandwidth evaluation in urban environment for PCS microcells, *in Proc. IST'02*, 508-512, (2002).
10. C. Christodoulou, and M. Georgiopoulos, *Applications of Neural Networks in Electromagnetics* (Artech House, 2001).
11. R. Janaswamy, Angle and time of arrival statistics for the Gaussian scatter density model, *IEEE Trans. Wireless Commun.*, **1**(3), 488-497 (2002).
12. H. Hu, V. Kukshya, and T. S. Rappaport, Spatial and temporal characteristics of 60-GHz indoor channels, *IEEE J. Select. Areas Commun.*, **20**(3), 620-630 (2002).